Available online at www.sciencedirect.com
SCIENCE DIRECT®
PERGAMON
International Journal of Heat and Mass Transfer 46 (2003) 3429–3440
International Journal of HEAT and MASS TRANSFER
www.elsevier.com/locate/ijhmt

Numerical analysis of the transient turbulent flow in a fuel oil storage tank

Nurten Vardar *

Department of Marine Engineering, Faculty of Mechanical Engineering, Yildiz Technical University, Istanbul 80750, Turkey

Received 18 July 2002; received in revised form 10 February 2003

Abstract

The filling process of a fuel oil storage tank containing a higher temperature fuel oil is numerically analysed. A k–ε model, which is developed by some modifications to those existing in the literature, is employed in order to take into account the turbulent effect for low-*Re* flow phenomena. A transient stream function–vorticity formulation is used for predicting streamlines and temperature distribution. The streamlines, the isotherms and the transient average temperature variations are presented for three different inflow velocities and for three different cases of heating.

1. Introduction

The quality of heavy fuel oil used in Diesel engines onboard ships and in power stations varies worldwide. Changes in refinery processes, which led to use of low-grade heavy fuel oils, have drastically changed the requirements placed on the fuel treatment systems. There is an increased demand for efficient cleaning in order to achieve reliable and economical operation of Diesel engines burning heavy fuel oils that include higher sludge content, more catfines and other harmful solid particles. The fuel treatment systems include heaters, filters, separators, pumps and settling and daily service tanks. The main purpose of using of settling tanks from cleaning aspects are to act as a buffer tank, to provide a constant temperature and to settle and drain gross water contamination.

The temperature in the tank should not be below 50–60 °C, otherwise the fuel oil may not be pumpable. On the other hand according to the classification societies, the storage temperature of fuel oil should be 10 °C at least below the flash point of the oils. Because of that it is important to maintain a constant cleaning temperature, and temperature control should be installed to minimise the temperature fluctuations in the settling tank. Due to the potential risk of thermal stratification problem in the tank and too low temperature at the suction point for the feed pump the place of the inlet port of the tanks are important as well.

The stratification of two fluids at different temperature is an important consideration in the design of thermal storage tanks In recent years considerable research efforts have been devoted to the study of thermal behaviour of the stratified fluids in thermal storage tanks especially in solar energy domain. Gari and Loehrke [1] described an inlet manifold for introducing arbitrary liquid temperature into a tank and developed a one-dimensional analytical model of the manifold. Baines et al. [2] investigated the effects of horizontal inflow into a rectangular tank for the case of a multiport manifold source spanning the bottom edge of the tank. Abu Hamdan et al. [3] carried out an experimental study to evaluate the performance of a stratified tank under variable inlet temperature conditions. They used a new inlet design and compared it with the most widely used conventional inlets. They found that devices of the kind used in their study offer no advantages over the conventional inlets under variable inlet temperature conditions. Nakos [4] analysed the flow of the gravity current before it reaches the end wall of the tank and compared the results obtained from the formulations with the experimental data.

* Tel.: +90-212-2597070x2312; fax: +90-212-2582157.
E-mail address: vardar@yildiz.edu.tr (N. Vardar).

0017-9310/03/$ - see front matter
doi:10.1016/S0017-9310(03)00145-5

Nomenclature

B	width of tank, buoyancy production/destruction of k
$C_{1,3}$	constants, Eq. (15)
$C_{\mu,2}$	dimensionless factors, Eqs. (12) and (13)
$C_{\mu_0,2_0}$	constants, Eq. (15)
D	depth from the fuel oil surface
E	dimensionless rate of dissipation of turbulence kinetic energy
g	gravity acceleration
Gr	Grashof number
h	height of inlet port
k	turbulence kinetic energy
K	dimensionless turbulence kinetic energy
L	height of tank
Pr	Prandtl number
Re	Reynold number
Re^*	Reynold number based on eddy viscosity
R_F	flux Richardson number
S	turbulence kinetic energy due to Reynold shear stress, Table 1
t	time
T	temperature
ΔT	$T_i - T_0$
u, v	horizontal and vertical velocities
U, V	dimensionless horizontal and vertical velocities
x, y	horizontal and vertical coordinates
X, Y	dimensionless horizontal and vertical coordinates

Greek symbols

α	thermal diffusivity
β	volumetric coefficient of expansion
ε	rate of dissipation of turbulence kinetic energy
η	kinematic viscosity
γ	startup function, Eq. (20)
ρ	density
θ	dimensionless temperature
$\sigma_{\varepsilon,k}$	constants, Eq. (15)
τ	dimensionless time
τ_0	dimensionless start uptime
ω	vorticity
Ω	dimensionless vorticity
Ψ	dimensionless stream function

Subscripts

i	initial
0	inflow
t	turbulent
ave_1	average (1D)
ave_2	average (2D)

Some of the investigators focused on the thermal behaviour of cylindrical storage tanks [5–9]. Homan and Soo [10,11] modelled the transient stratified flow into a chilled-water storage tank for laminer flow conditions and in Cartesian coordinates. They presented numerical solutions for the flow field transients with a single jet of cold liquid entering horizontally at the bottom of a tall tank initially filled with hotter liquid and for the efficiency of a stratified chilled-water storage tank with one inlet and one outlet. Al-Najem and El-Refaee [12] investigated the transient behaviour of thermal stratification in storage systems by developing a computer code on Chapeau–Galerkin integral formulation. Eames and Norton [13] studied the effect of tank geometry on thermally stratified sensible heat storage. They developed a finite volume based transient three-dimensional model and they validated the model by comparing with experimental results. Mo and Miyatake [14] numerically analysed the transient turbulent flow field in thermally stratified water tank. They employed the Quickest

Table 1
Definitions for Γ, B and S

Equation	Γ	B	S
Ω	$\frac{1}{Re}+\frac{1}{Re^*}$	–	–
θ	$\frac{1}{RePr}+\frac{1}{Re^*Pr_t}$	–	–
K	$\frac{1}{Re}+\frac{1}{Re^*\sigma_k}$	$\frac{1}{Re^*Pr_t}\frac{Gr}{Re^2}\frac{\partial\theta}{\partial Y}$	$\frac{1}{Re^*}\left\{2\left[\left(\frac{\partial U}{\partial X}\right)^2-\left(\frac{\partial V}{\partial Y}\right)^2\right]+\left(\frac{\partial U}{\partial Y}+\frac{\partial V}{\partial X}\right)^2\right\}$
E	$\frac{1}{Re}+\frac{1}{Re^*\sigma_\varepsilon}$	$\frac{1}{Re^*Pr_t}\frac{Gr}{Re^2}\frac{\partial\theta}{\partial Y}$	$\frac{1}{Re^*}\left\{2\left[\left(\frac{\partial U}{\partial X}\right)^2-\left(\frac{\partial V}{\partial Y}\right)^2\right]+\left(\frac{\partial U}{\partial Y}+\frac{\partial V}{\partial X}\right)^2\right\}$

(Quick with estimating streaming terms) method to solve the energy equation and used the k–ε model to account for the turbulent effect. They compared the results with the existing experimental results. Cai and Stewart [15] investigated the mixing process that occurs when a cold fluid flows in to a two-dimensional tank containing a warmer fluid. They developed a numerical model to simulate the turbulent flow in the tank and used Prandtl–Kolmogorov formulation to take the turbulent effects into account. They presented streamline and isotherm results for variation of Reynold numbers, tank size relative to inlet size and Archimedian numbers. As mentioned before the existing literature in this domain has focused considerable attention on the thermal stratification in thermal water storage tanks. A few studies have been reported for the case of different fluids such as liquid natural gas or oil [16–19].

The purpose of this present work is to investigate the transient turbulent flow field and thermal behaviour of the fuel oil in the tank where the viscosity is higher than water's. For this aim the flow and the temperature field are obtained by using the formulations from the existing literature [14,15,20,21] with applying some modifications in turbulent kinetic energy dissipation equation which are explained in detail in this work.

2. Mathematical model

Although many of the tank designs require a full three-dimensional approach, since the inflow velocities are low and thus a little turbulent mixing occurs around the inlet region a two-dimensional approximation is a reasonable assumption for the present study. Moreover modelling of the flow to bring out the three-dimensional details of the flow is very computer resources intensive, and therefore a simplified two-dimensional geometry is adopted as shown in Fig. 1. The height of the inlet is h and the height and width of the tank are L and B, respectively. The side and bottom walls and fluid surfaces are assumed to be thermally insulated and the tank is filled with hot fuel oil at an initial temperature. Cold fuel oil always at a lower temperature than the fuel oil in the tank enters at the lower corner of the tank.

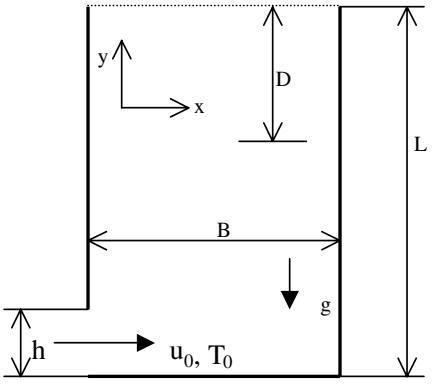

Fig. 1. Geometry and coordinates of the tank.

The governing equations describing transient and turbulent flow of viscous, incompressible fluid in the tank are continuity, momentum, energy, turbulent kinetic energy and dissipation rate of turbulent kinetic energy equations. The turbulent kinetic energy dissipation equation is modified form of the equation that is used by Mo and Miyatake in [14]. The modification of this equation is achieved according to the Launder and Spalding's [20] low-Reynold k–ε model. Boussinesq approximation, $\rho = \rho_0[1-\beta(T-T_0)]$, utilised for the buoyancy terms in these equations which assumes that the physical properties other than the density appearing in the buoyancy terms are constant [22]. Dimensionless equations in stream function–vorticity formulations are given as follows:

$$\frac{\partial \Omega}{\partial \tau}+\frac{\partial (U\Omega)}{\partial X}+\frac{\partial (V\Omega)}{\partial Y} = \frac{\partial^2}{\partial X^2}(\Gamma\Omega)+\frac{\partial^2}{\partial Y^2}(\Gamma\Omega)+\frac{Gr}{Re^2}\frac{\partial \theta}{\partial X}+S \tag{1}$$

$$\frac{\partial \theta}{\partial \tau}+\frac{\partial (U\theta)}{\partial X}+\frac{\partial (V\theta)}{\partial Y} = \frac{\partial}{\partial X}\left(\Gamma\frac{\partial \theta}{\partial X}\right)+\frac{\partial}{\partial Y}\left(\Gamma\frac{\partial \theta}{\partial Y}\right) \tag{2}$$

$$\frac{\partial K}{\partial \tau}+\frac{\partial (UK)}{\partial X}+\frac{\partial (VK)}{\partial Y} = \frac{\partial}{\partial X}\left(\Gamma\frac{\partial K}{\partial X}\right)+\frac{\partial}{\partial Y}\left(\Gamma\frac{\partial K}{\partial Y}\right)+S+B-E \tag{3}$$

$$\frac{\partial E}{\partial \tau}+\frac{\partial (UE)}{\partial X}+\frac{\partial (VE)}{\partial Y} = \frac{\partial}{\partial X}\left(\Gamma\frac{\partial E}{\partial X}\right)+\frac{\partial}{\partial Y}\left(\Gamma\frac{\partial K}{\partial Y}\right)+C_1\frac{E}{K}(S+B)(1+C_3R_F)-C_2\frac{E^2}{K} \tag{4}$$

$$\nabla^2\Psi = -\Omega \tag{5}$$

$$R_F = -\frac{B}{B+S} \tag{6}$$

Eqs. (1)–(5) are written in terms of the following dimensionless variables:

$$X,Y=\frac{x,y}{h},\quad U,V=\frac{u,v}{u_0},\quad \tau=\frac{u_0 t}{h} \tag{7}$$

$$K=\frac{k}{u_0^2},\quad E=\frac{h}{u_0^3}\varepsilon,\quad \theta=\frac{T-T_0}{\Delta T},\quad \Omega=\frac{\omega}{u_0}h \tag{8}$$

$$Re=\frac{u_0}{\eta}h,\quad Re^*=\frac{u_0}{\eta_t}h=\frac{1}{C_\mu}\frac{E}{K^2} \tag{9}$$

$$Pr = \frac{\eta}{\alpha}, \quad Pr_t = 0.75 + \frac{0.708}{\log Pr + 2.83}, \quad Gr = \frac{g\beta\Delta T h^3}{\eta^2} \tag{10}$$

The actual variables on the right-hand side of Eqs. (7)–(10) are listed in the nomenclature. The turbulent viscosity η_t in Eq. (9) is expressed as follows:

$$\eta_t = C_\mu \frac{k^2}{\varepsilon} \tag{11}$$

Re^* is the Reynold number based on eddy viscosity [21], Pr_t is the turbulent Prandtl number, which is determined using the empirical formulation from [23]. Dimensionless factors C_2 and C_μ in Eqs. (4), (9) and (11) are functions of the turbulence Reynold number Re_t [20].

$$C_\mu = C_{\mu_0} \exp\left[\frac{-2.5}{(1 + Re_t/50)}\right] \tag{12}$$

$$C_2 = C_{2_0}[1.0 - 0.3 \exp -Re_t^2] \tag{13}$$

$$Re_t = Re\frac{K^2}{E} \tag{14}$$

The values of the numerical constants appearing in above equations are given as follows [14,20]:

$$\begin{aligned} &C_1 = 1.44, \quad C_3 = 0.8, \quad \sigma_k = 1.0 \\ &\sigma_\varepsilon = 1.3, \quad C_{2_0} = 1.92, \quad C_{\mu_0} = 0.09 \end{aligned} \tag{15}$$

The dimensionless initial and boundary conditions are shown as below:

At the inlet $X = 0$ and $0 \leqslant Y \geqslant h/h$ [14]

$$\begin{aligned} &U(Y) = \frac{2(h/h - Y)Y}{(h/h)^2}, \quad \Psi = \int_0^{h/h} U(Y)\,dY \\ &\Omega = -\frac{\partial U(Y)}{\partial Y}, \quad K = 0.01, \quad \frac{\partial E}{\partial X} = 0 \end{aligned} \tag{16}$$

At the fluid surface $Y = L/h$ and $0 \leqslant X \geqslant B/h$

$$U = E = K = \Omega = \frac{\partial V}{\partial Y} = \frac{\partial \theta}{\partial Y} = \frac{\partial \Psi}{\partial Y} = 0 \tag{17}$$

At the bottom wall $Y = 0$ and $0 \leqslant X \geqslant B/h$

$$U = V = \Psi = \frac{\partial \theta}{\partial Y} = 0 \tag{18}$$

At the right wall $X = B/h$ and $0 \leqslant Y \geqslant L/h$

$$U = V = \Psi = 0, \quad \Omega = -\frac{\partial^2 \Psi}{\partial X^2} \tag{19}$$

At the left wall $X = 0$ and $h/h \leqslant Y \geqslant L/h$

$$U = V = 0, \quad \Omega = -\frac{\partial^2 \Psi}{\partial X^2}, \quad \Psi = \gamma(\tau, \tau_0) \tag{20}$$

γ appearing in Eq. (20) is the startup function used for ramping the inlet boundary condition on velocity from its initial condition to its steady-state value over a dimensionless time period of 0.2, which is defined as follows [11]:

$$\gamma(\tau, \tau_0) = \left\{ \begin{array}{ll} (\tau/\tau_0^2)^2(3 - 2\tau/\tau_0) & \tau/\tau_0 \leqslant 1 \\ \Psi(0, h/h) & \tau/\tau_0 \geqslant 1 \end{array} \right\} \tag{21}$$

The dimensionless temperature value on the vertical walls is taken to be 1 for the heating case, while the gradient of temperature values are assumed to be zero for the non-heating case. Since the low-Reynold number k–ε model is used to calculate the turbulent effects, there is no need for wall function to account for the large damping of turbulence in the wall region. The turbulent kinetic energy and gradient of dissipation are prescribed as zero at the solid surfaces.

The initial conditions are

$$U = V = K = E = \Psi = \Omega = 0, \quad \theta = 1 \tag{22}$$

The mathematical model is solved by a finite differences procedure described by Chow [22]. At any time instant the vorticity, the temperature, the turbulent kinetic energy and the dissipation distributions are obtained from conditions at the previous time step. Upwind and central differencing scheme is used to approximate the time derivatives. Stream function is computed based on vorticity distribution by solving Eq. (5) with the successive over relaxation method. Velocity components are calculated from the known stream functions.

The two-dimensional computational region as shown in Fig. 1 is an open top rectangular tank and it has a height of 20 times the dimension of the inlet opening. For the simulations 21×41 uniform grid sizes are chosen after performing the grid independency tests. In order to investigate the effect of grid sizes, three sets of grids 21×41, 41×81 and 51×101 are used. In order to compare the computational results for the three grid sizes the average temperatures are plotted versus the grid numbers in Fig. 2a. The average temperature for the two-dimensional tank domain at any time is calculated according to the following

$$\theta_{ave_2} = \frac{1}{(L/h)(B/h)} \int_0^{B/h} \int_0^{L/h} \theta\,dX\,dY \tag{23}$$

During the transient process grid size effect is evident but not too significant. The deviations between the average temperatures depending on the time can be seen in Fig. 2b. Even for the grid sizes of $21 \times 41/51 \times 101$, the maximum deviation between results is less than 1.3%. Therefore, 21×41 grid size is selected in order to save the computing time.

2.1. Validation of the method

The configuration of the tank, which is used in simulations is shown in Fig. 1. First in order to check the

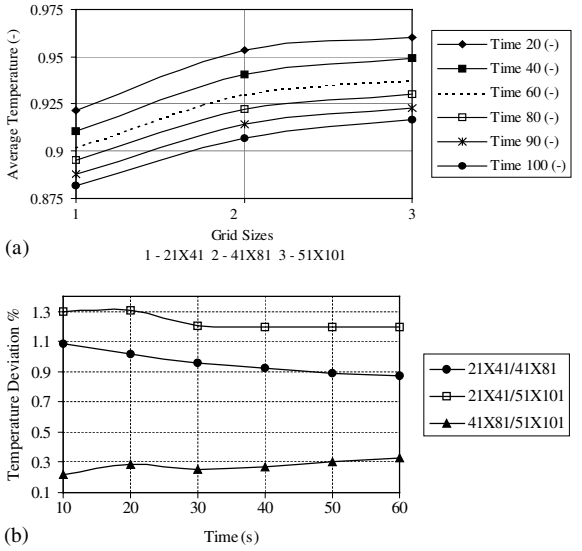

Fig. 2. (a) Effect of grid size on transient average temperatures. (b) Deviations between average temperatures.

accuracy of the present method, the problem considered by Cai and Stewart [15] is solved. The dimensions of the tank and most of other computational parameters are taken to be the same as those used by Cai and Stewart. For the validation of the method, the results of the present study are compared with the results of reference study. In the simulation, which is carried out for the validation of the method, the tank is assumed to be filled with hot water at an initial temperature. The inlet fluid flow is assumed to be colder than the tank fluid and the difference between the inlet temperature and the initial temperature of the tank fluid is 15 °C. Fig. 3a and b shows that the results of the present model are in good agreement with those given by Cai and Stewart [15].

3. Results and discussion

The tank is assumed to be filled with stagnant fuel oil at 60 °C. The fuel oil entering into the tank is at 40 °C from the beginning of the process. Kinematic viscosity of the fuel oil is 3.75×10^{-4} m^2/s and Prandtl number is 10400 at inflow temperature. The inlet fluid opening height is 0.1 m, the inflow velocities are 0.25, 0.5 and 1 m/s and the inflow Reynold numbers related to these inflow velocities which are calculated according to Eq. (9) are 67, 133 and 266, respectively. The values of the parameter of Gr/Re^2, which is an important parameter for the transient turbulent flow in thermal storage tanks, are determined by using the definition of the Grashof number in Eq. (10). These Gr/Re^2 values are 0.218 for $Re = 67$, 0.055 for $Re = 133$ and 0.0137 for $Re = 266$. The dimensionless time step is chosen to be 0.05. In order to examine the effects of the inflow velocity and heating condition on the transient thermal behaviour of the tank the average temperatures are calculated at three different depths of the tank. The average temperature at

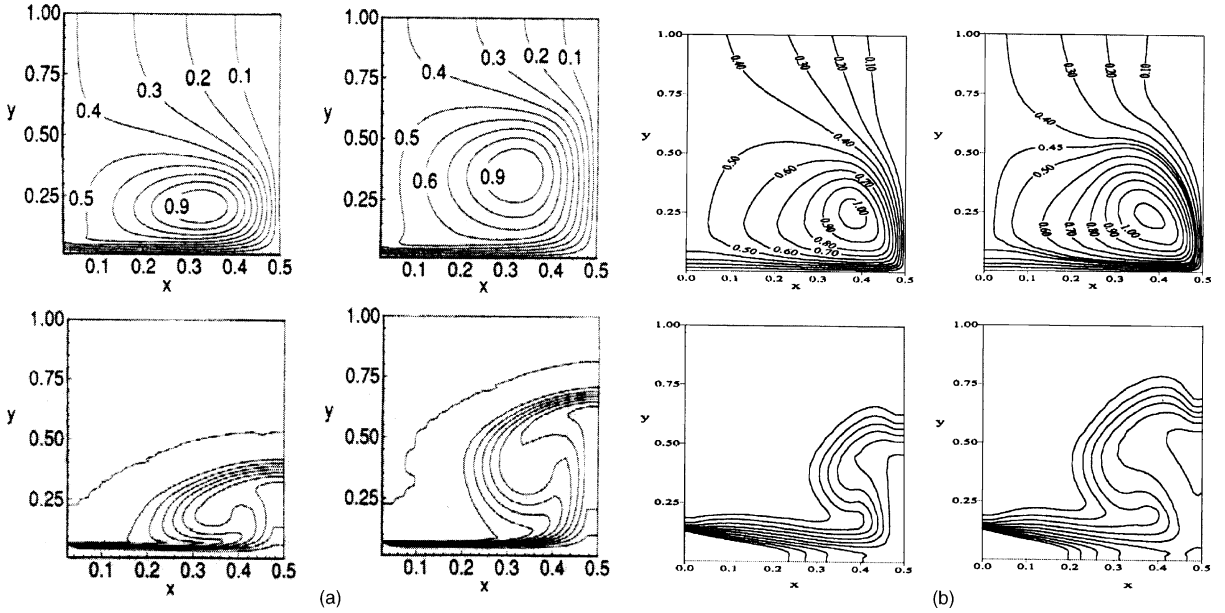

Fig. 3. (a) Streamlines (top) and isotherms (bottom) of the reference study [15], $T = 2$ (left), $T = 3$ (right). (b) Streamlines (top) and isotherms (bottom) of the present study $\tau = 40$ (left), $\tau = 60$ (right).

horizontal plane at any depth of the tank is defined as follows:

$$\theta_{\mathrm{ave}_1} = \frac{1}{B/h}\int_0^{B/h} \theta \, \mathrm{d}X \tag{24}$$

The average temperatures are calculated at two depths ($D/L = 0.5$, $D/L = 0.75$) and at the fluid surface. On the other hand the streamlines and isotherms, which constitute the means of comparison between these different conditions, are also calculated. The sufficient dimensional simulation times to show the transient average temperature variations are 250 s and to show the initial mixing of cold and hot fuel oil in the lower region of the tank are 60 s for all Re numbers, Gr/Re^2 parameters and all heating conditions. All of the calculations are made in dimensionless form in this study. The dimensionless time depends on the inflow velocity. The dimensionless simulation times used in this study are 625, 1250 and 2500 for different inflow velocities 0.25, 0.5 and 1.0 m/s, respectively. Although these dimensionless times appear to be different from each other, they are in fact the same as each other for all of the inflow velocities. It should be noted that all these dimensionless simulation times correspond to the dimensional time of 250 s. Therefore, in order to avoid from confusion and to observe the transient thermal behaviour of the tank more easily, the dimensional transient average temperatures are plotted versus the dimensional time.

3.1. Effect of Reynold number on the transient average temperature variations

In order to compare the thermal behaviours of the tank the dimensional transient average temperatures are plotted versus the dimensional time. The variations of average temperatures in two depths of the tank ($D/L = 0.5$ and $D/L = 0.75$) and on the fluid surface ($D/L = 1$) for three different Reynolds numbers are shown in Figs. 4–6. For all Reynold numbers the average temperatures at each depth decrease from 60 °C (hot fuel oil temperature) to 40 °C (cold fuel oil temperature) after a lag time that depends on Reynold number.

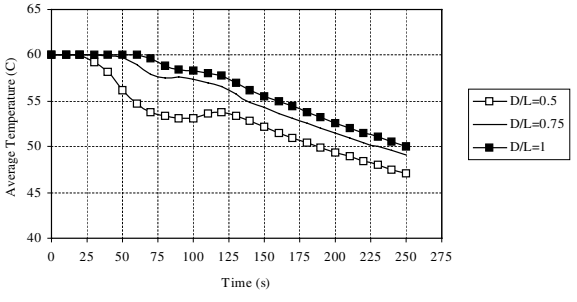

Fig. 4. Transient average temperature variations at three depths at $Re = 67$, $Gr/Re^2 = 0.218$.

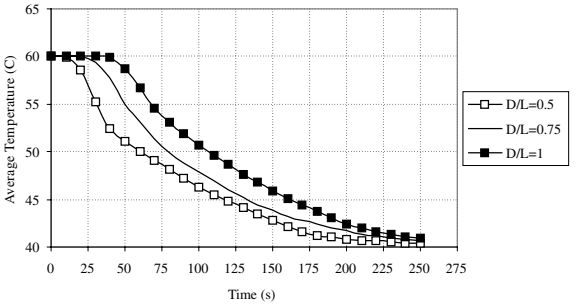

Fig. 5. Transient average temperature variations at three depths at $Re = 133$, $Gr/Re^2 = 0.055$.

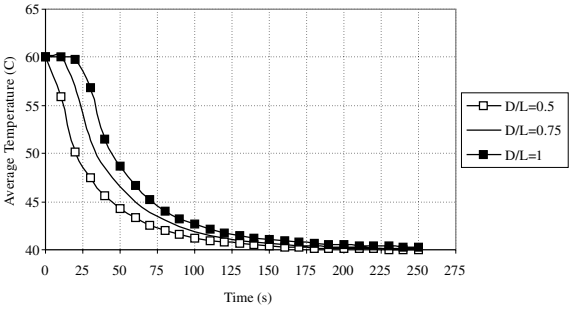

Fig. 6. Transient average temperature variations at three depths at $Re = 266$, $Gr/Re^2 = 0.0137$.

As is shown in Fig. 4, the lag time at $D/L = 0.75$ and at the fluid surface is more than 60 s, at $D/L = 0.5$ the lag time is about 25 s for the case of $Re = 67$ and $Gr/Re^2 = 0.218$. As soon as the lag time ends, the transient average temperature decreases rapidly till the end of 100 s and it slightly increases and then begins to decrease slowly again for all cases. The average temperature at the fluid surface decreases to 50 °C after the time period of 250 s. Fig. 5 shows the transient average temperatures at $Re = 133$, $Gr/Re^2 = 0.055$. The average temperatures decrease rapidly compared to the first case. The lag time is less than 50 s for each depth and the average temperatures at the end of 250 s are below 42 °C. As can be seen from Fig. 6 in the case of Re number of 266 and Gr/Re^2 parameter of 0.0137 the lag times at each depth are less than 20 s and the average temperatures decrease rapidly to the inflow temperature level at each depth of the tank.

3.2. Effect of heating conditions on the transient average temperature variations

The effect of the heating conditions on the transient average temperature variation in the fuel oil tank is investigated. A constant temperature condition is applied either to the left-hand wall or right-hand wall. The

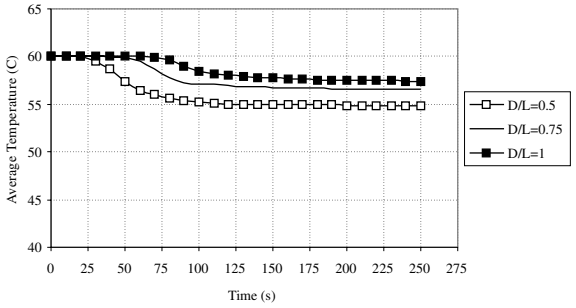

Fig. 7. Transient average temperature variations at three depths in the case of the hot left-hand wall at $Re = 67$, $Gr/Re^2 = 0.218$.

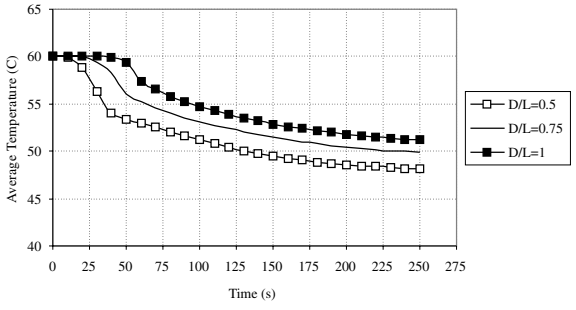

Fig. 8. Transient average temperature variations at three depths in the case of the hot left-hand wall at $Re = 133$, $Gr/Re^2 = 0.055$.

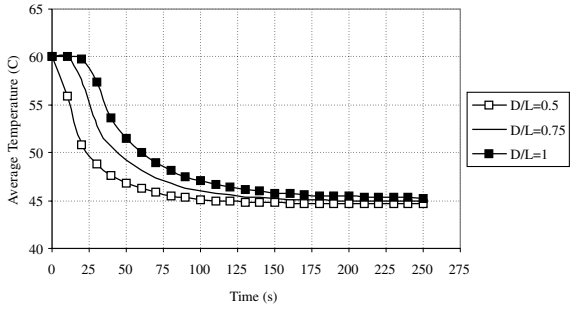

Fig. 9. Transient average temperature variations at three depths in the case of the hot left-hand wall at $Re = 266$, $Gr/Re^2 = 0.0137$.

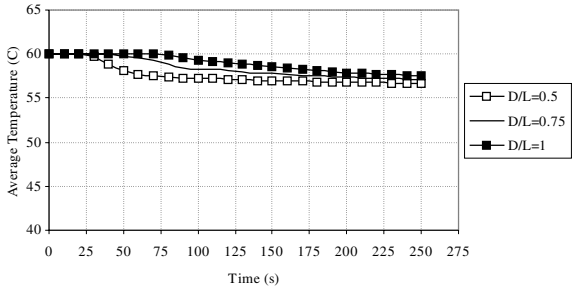

Fig. 10. Transient average temperature variations at three depths in the case of hot right-hand wall at $Re = 67$, $Gr/Re^2 = 0.218$.

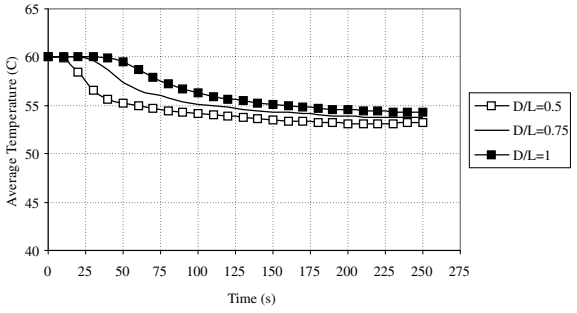

Fig. 11. Transient average temperature variations at three depths in the case of hot right-hand wall at $Re = 133$, $Gr/Re^2 = 0.055$.

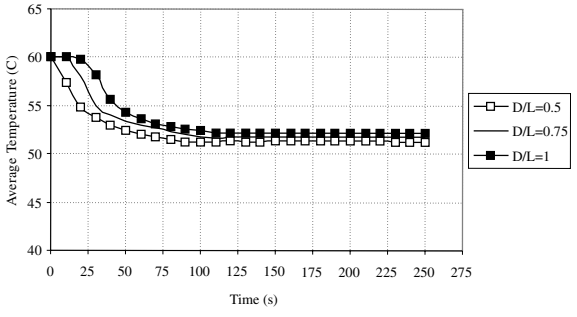

Fig. 12. Transient average temperature variations at three depths in the case of hot right-hand wall at $Re = 266$, $Gr/Re^2 = 0.0137$.

other walls and fuel oil surface are assumed to be thermally isolated. The average temperature variations in the case of the hot left-hand wall for the same Reynold numbers as those used in the previous section are shown in Figs. 7–9. As can be seen from these figures the lag times for all Reynold numbers are the same as the lag times of the non-heating tank condition. In the case of $Re = 67$ and $Gr/Re^2 = 0.218$ the average temperatures decrease very slowly after the lag time and they stay constant between 55 and 60 °C after 125 s. In the case of $Re = 133$ and $Gr/Re^2 = 0.055$ the average temperatures are about 50 °C after 250 s. In the case of $Re = 266$ and $Gr/Re^2 = 0.0137$ the average temperatures at each depth decrease rapidly down to 45 °C in a period of time of 80 s and they stay constant at this level. As can be seen from Figs. 10–12, in the case of the hot right-hand wall

conditions the average temperatures at each depth of the tank show a little drop after the lag time and they stay constant above 50 °C for each Reynold number.

3.3. Transient flow and temperature fields

For different Reynold numbers and heating conditions, the computed results are transiently visualised with a series of streamlines and isotherms. The intervals for the streamlines and for the isotherms are set to be 0.2 and 0.1, respectively. Fig. 13 shows instantaneous streamlines and isotherms for the lowest Reynold number and the highest Gr/Re^2 parameter considered in this study ($Re = 67$ and $Gr/Re^2 = 0.218$). The streamlines in Fig. 13 show that the cold fuel oil enters into the tank, impinges upon the right-hand wall and changes its direction to the left-hand wall at $t = 10$ s. After arriving the left-hand wall it begins to return to the right-hand wall at $t = 20$ s. A second vortex begins to form in the tank and the fuel oil impinges the right-hand wall again at $t = 50$ s. In the transient isotherms (solid lines), it is found that the cold and the hot fuel oil are separated by a thermocline and it moves up as time elapses. Apparently the thermocline isolates the flow fields above and below itself very effectively. Above the thermocline, the streamlines indicate that the flow is nearly uniform. The region below the thermocline is filled with recirculation cells.

In Fig. 14 streamline and isotherm results for Re of 133 and Gr/Re^2 of 0.055 show the flow field in the tank for the first 30 s are nearly the same as the result in Fig. 13. But the second vortex forms at $t = 40$ s and gets smaller as time elapses. The thermocline forms in that case as well, however the temperatures in the tank decrease in a shorter time period and thermocline moves up more rapidly compared to the first case.

As can be seen from Fig. 15 in the case of $Re = 266$ and $Gr/Re^2 = 0.0137$ the thermal mixing occurs preventing the formation of a thermocline especially at lower portion of the tank. The stream forms a bigger vortex at this region than the previous two cases. This vortex which induces further turbulent mixing, produces an irregular temperature distribution. The maximum dimensionless temperature at $t = 60$ s is 0.30 which is the smallest maximum temperature value among the results of three cases at $t = 60$ s.

The effects of heating conditions on the streamlines and the isotherms are shown in Figs. 16–19. In the case of a constant temperature on the left-hand wall of the tank the streamlines and the isotherms for a Reynold number of 67 and Gr/Re^2 parameter of 0.218 at $t = 60$ s can be seen in Fig. 16. It is seen from Fig. 16 that the streamlines and the isotherms in these conditions are nearly the same as the results of the non-heating tank condition as mentioned before. The streamlines and the isotherms under the constant temperature conditions on

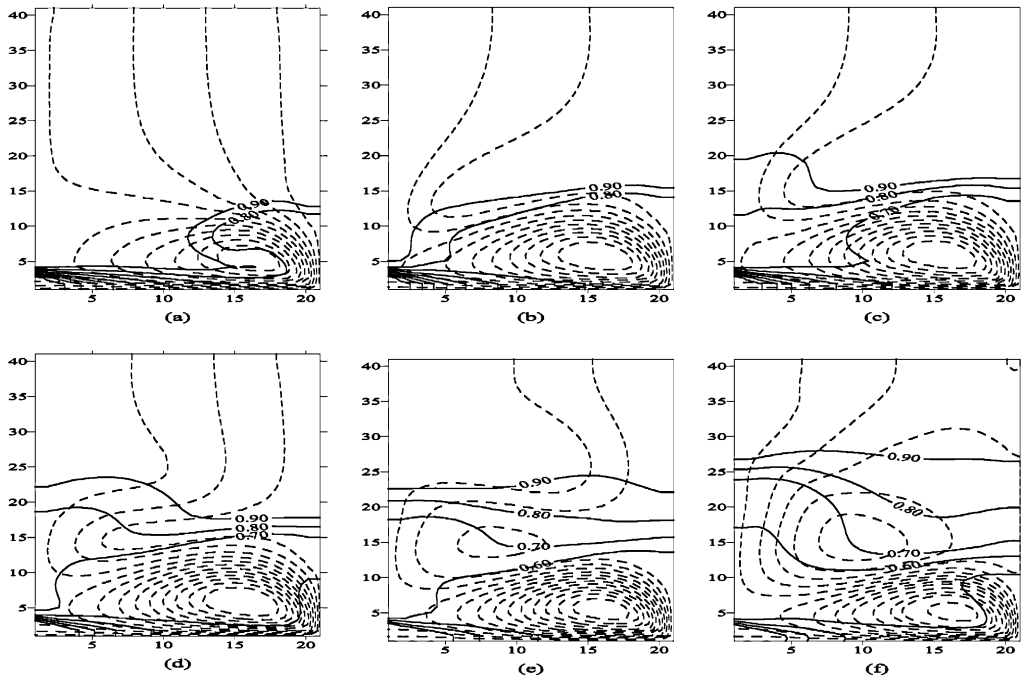

Fig. 13. Transient streamlines (dashed lines) and isotherms (solid lines) at $Re = 67$, $Gr/Re^2 = 0.218$, (a) $t = 10$ s, (b) $t = 20$ s, (c) $t = 30$ s, (d) $t = 40$ s, (e) $t = 50$ s, (f) $t = 60$ s.

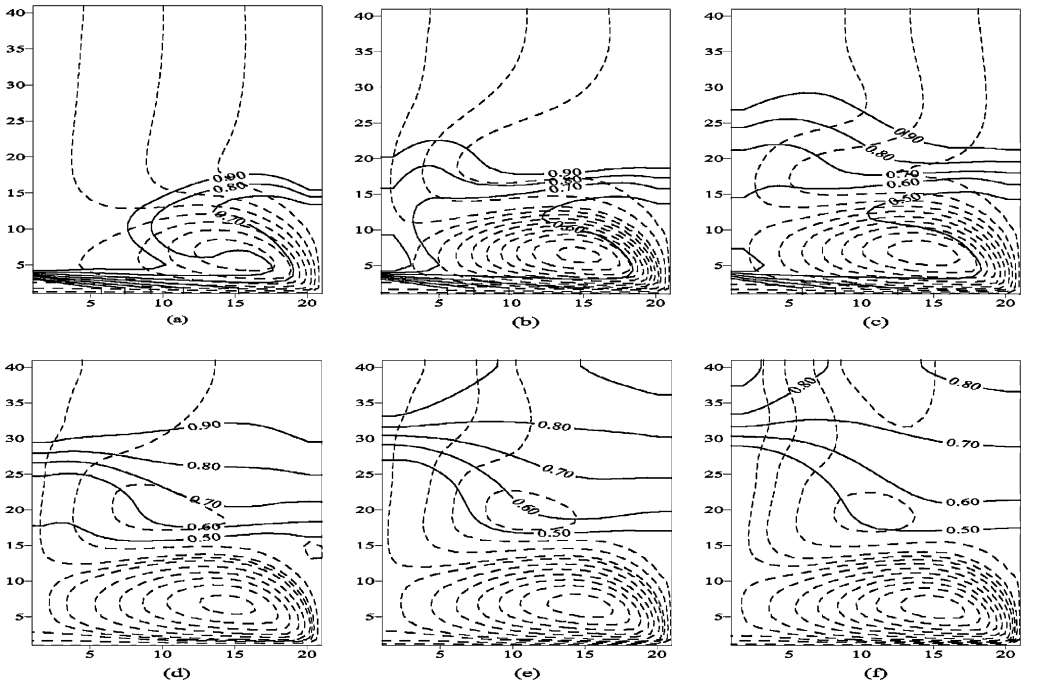

Fig. 14. Transient streamlines (dashed lines) and isotherms (solid lines) at $Re = 133$, $Gr/Re^2 = 0.055$, (a) $t = 10$ s, (b) $t = 20$ s, (c) $t = 30$ s, (d) $t = 40$ s, (e) $t = 50$ s, (f) $t = 60$ s.

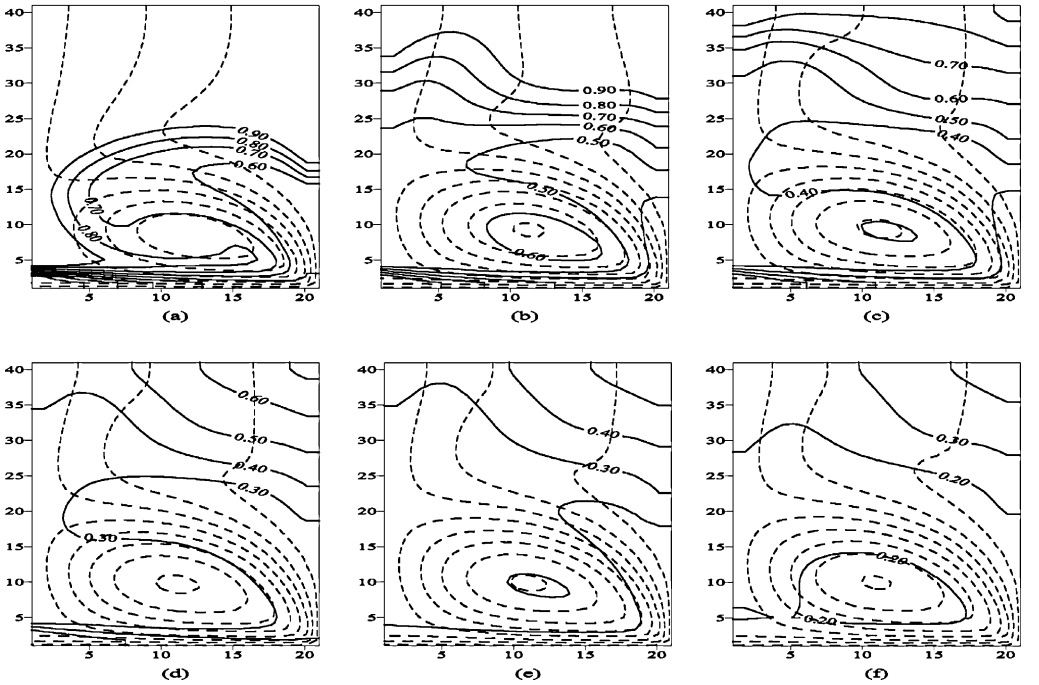

Fig. 15. Transient streamlines (dashed lines) and isotherms (solid lines) at $Re = 266$, $Gr/Re^2 = 0.0137$, (a) $t = 10$ s, (b) $t = 20$ s, (c) $t = 30$ s, (d) $t = 40$ s, (e) $t = 50$ s, (f) $t = 60$ s.

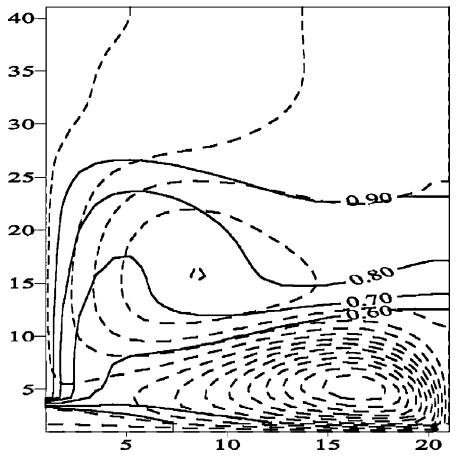

Fig. 16. Transient streamlines (dashed lines) and isotherms (solid lines) in the case of hot left-hand wall, at $Re = 67$, $Gr/Re^2 = 0.218$, $t = 60$ s.

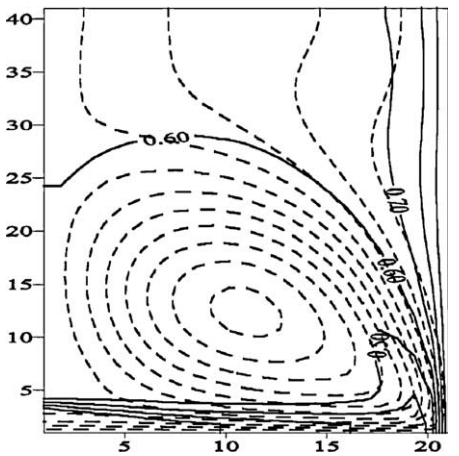

Fig. 18. Transient streamlines (dashed lines) and isotherms (solid lines) in the case of hot right-hand wall, at $Re = 67$, $Gr/Re^2 = 0.218$, $t = 60$ s.

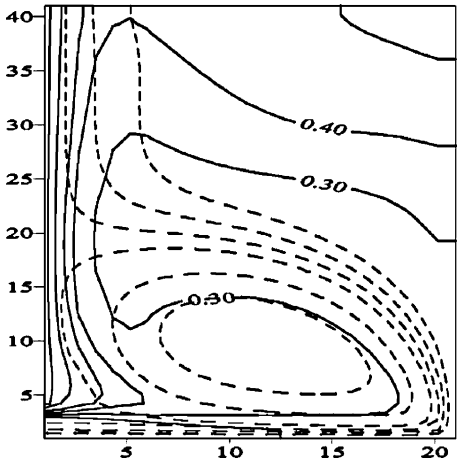

Fig. 17. Transient streamlines (dashed lines) and isotherms (solid lines) in the case of hot left-hand wall, at $Re = 266$, $Gr/Re^2 = 0.0137$, $t = 60$ s.

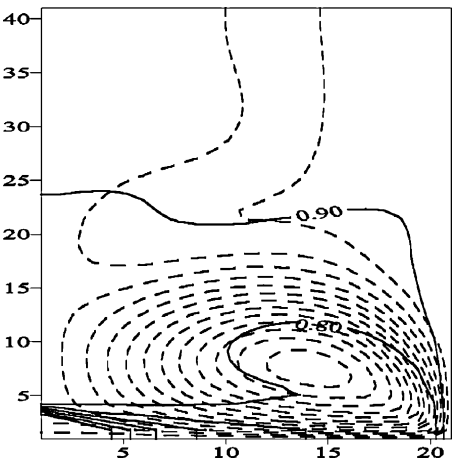

Fig. 19. Transient streamlines (dashed lines) and isotherms (solid lines) in the case of hot right-hand wall, at $Re = 266$, $Gr/Re^2 = 0.0137$, $t = 60$ s.

the left-hand wall of the tank for a Reynold number of 266 and Gr/Re^2 parameter of 0.0137 are shown in Fig. 17. It can be seen that the vortex formed in the tank is as big as the one in the non-heated tank, but the streamlines at the upper portion of the tank are close to the hot wall of the tank at $t = 60$ s. As for the isotherms it can be said that there is no important effect of heating of the left-hand wall of the tank except on the temperature distribution in the region close to the hot wall. The temperature along the tank height is similar to the temperature distribution in the non-heating tank. The streamlines and the isotherms in the tank with heated right-hand wall, at $t = 60$ s when $Re = 67$ and $Re = 266$ are shown in Figs. 18 and 19, respectively. As can be seen from Fig. 18 the streamlines are different from the results of all the other cases, which are previously investigated. Only an intensive vortex forms and a second vortex does not appear in the tank. The flow above the vortex is more uniform than expected and the streamlines do not get close to the hot right-hand wall. The isotherms are different from all of the other cases considered so far in this study. A thick temperature band forms between the vortex center and the vortex boundary and the dimensionless temperatures near the vortex center and near the vortex boundary are 0.8 and 0.9, respectively.

It appears in Fig. 19 in the case of $Re = 266$ the most intensive vortex forms compared to the each of the cases

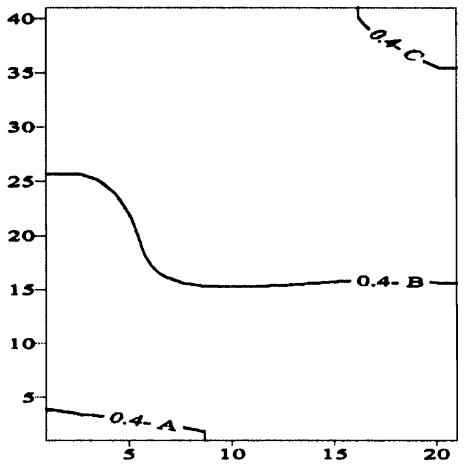

Fig. 20. Location of the 0.4 isotherms in the non-heating tank at, $t = 60$ s (A—$Re = 67$, B—$Re = 133$ and C—$Re = 266$).

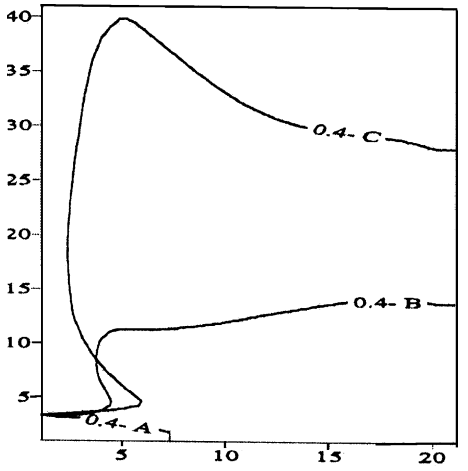

Fig. 21. Location of the 0.4 isotherms in the case of hot left-hand wall at, $t = 60$ s (A—$Re = 67$, B—$Re = 133$ and C—$Re = 266$).

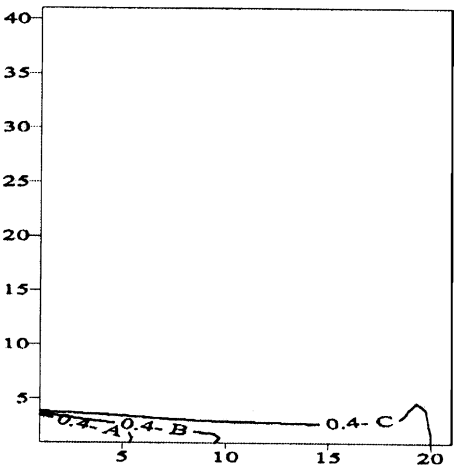

Fig. 22. Location of the 0.4 isotherms in the case of hot right-hand wall, at $t = 60$ s (A—$Re = 67$, B—$Re = 133$ and C—$Re = 266$).

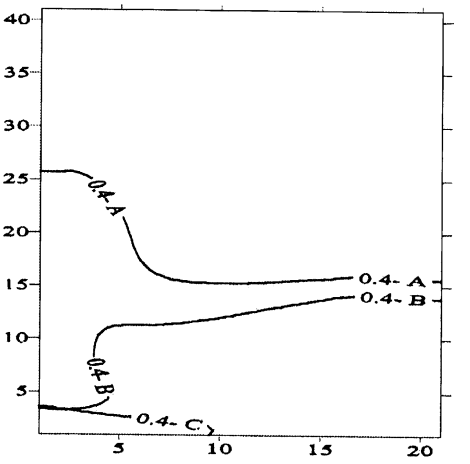

Fig. 23. Location of the 0.4 isotherms in the cases of different heating conditions, at $Re = 133$ and $t = 60$ s (A—non-heating, B—hot left-hand wall, C—hot right-hand wall).

taken into account. Although the flow above the vortex is uniform as in the case of $Re = 67$, the streamlines become closer to the hot right-hand wall. The isotherms are found to be different in comparison with the other cases. The temperature gradient develops nearly vertically rather than horizontally especially in the right-hand side of the tank. As mentioned earlier the temperature in the tank should not be below 50 °C. Therefore it is reasonable to illustrate the minimum temperature region in the tank. Minimum dimensionless temperature is chosen to be 0.4 according to Eq. (8), which corresponds to 48 °C. Fig. 20 shows the location of the 0.4 isotherms for three different Reynold numbers in the non-heating tank. Figs. 21 and 22 show the location of the 0.4 isotherms for the conditions of hot left-hand wall and the hot right-hand wall of the tank and for three different Reynold numbers, respectively. Fig. 23 shows the location of the 0.4 isotherm for three different heating conditions for the case of $Re = 133$. All of the results that appear in Figs. 20–23 are for $t = 60$ s.

4. Conclusions

In this work the filling process of a fuel oil storage tank containing a higher temperature fuel oil is modelled. The k–ε model is employed in order to account for

the turbulent effect. The flow and temperature fields and transient average temperature variations are obtained for three different Reynold numbers depending on inflow velocities and for three different Gr/Re^2 parameters characterising the buoyancy effect in the tank. The effects of two different heating conditions on the flow and temperature fields are also investigated. In the case of low inflow velocity ($u_0 = 0.25$ m/s), and for non-heating conditions the average temperatures at three depths are found to be 50 °C and below after a period of time of 250 s. Under the heating conditions from the right- or left-hand wall the average temperatures stayed as constant after $t = 100$ s at 55 °C and above, which is sufficient for the pumping of the fuel oil. For the other two inflow velocities (0.5 and 1 m/s) and heating conditions the average temperatures dropped to 50 °C and below except the case of heating of the right-hand wall of the tank. Only in that case for all inflow velocities the average temperatures stayed constant at the pumpable temperature limits after a time period of 100 s constant at the pumpable temperature limits.

References

[1] H.N. Gari, R.I. Loehrke, A controlled buoyant jet for enhancing stratification in a liquid storage tank, J. Fluids Eng. 104 (1982) 475–481.

[2] W.D. Baines, W.W. Martin, D.M. Smith, Development of stratification in a rectangular tank by horizontal flow, J. Fluids Eng. 105 (1983) 59–64.

[3] M.G. Abu Hamdan, Y.G. Zurigat, A.J. Ghajar, An experimental study of a stratified thermal storage under variable inlet temperature for different inlet design, Int. J. Heat Mass Transfer 35 (1992) 1927–1933.

[4] J.T. Nakos, The prediction of velocity and temperature profiles in gravity currents for use in chilled water storage tanks, J. Fluids Eng. 116 (1994) 83–90.

[5] K.A.R. İsmail, J.F.B. Leal, M.A. Zanardi, Models of liquid storage tanks, Energy 22 (1996) 805–815.

[6] A. Bouhdjar, A. Benkhelifa, Numerical study of transient mixed convection in a cylindirical cavity, Numer. Heat Transfer 31 (1997) 305–324.

[7] R.S. Robert, A numerical study of transient mixed convection in cylindirical thermal storage tanks, Int. J. Heat Mass Transfer 41 (1998) 2003–2011.

[8] M. Inallı, Design parameters for a solar heating system with an underground cylindrical tank, Energy 23 (1998) 1015–1027.

[9] S. Alizadeh, An experimental and numerical study of thermal stratification in a horizontal cylindirical solar storage tank, Solar Energy 66 (1999) 409–421.

[10] K.O. Homan, S.L. Soo, Model of the transient stratified flow into a chilled-water storage tank, Int. J. Heat Mass Transfer 40 (1997) 4367–4377.

[11] K.O. Homan, S.L. Soo, Laminer flow efficiency of stratified chilled-water storage tank, Int. J. Heat Fluid Flow 19 (1998) 69–78.

[12] N.M. Al-Najem, M.M. El-Refaee, A numerical study for the prediction of turbulent mixing factor in thermal storage tanks, Appl. Thermal Eng. 17 (1997) 1173–1181.

[13] P.C. Eames, B. Norton, The effect of tank geometry on thermally stratified sensible heat storage subject to low Reynolds number flows, Int. J. Heat Mass Transfer 41 (1998) 2131–2142.

[14] Y. Mo, O. Miyatake, Numerical analysis of the transient turbulent flow field in a thermally stratified thermal storage water tank, Numer. Heat Transfer 30 (1996) 649–667.

[15] L. Cai, W.E. Stewart Jr., Turbulent buoyant flows into a two dimensional storage tank, Int. J. Heat Mass Transfer 36 (1993) 4247–4256.

[16] S. Bates, D.S. Morrison, Modeling the behaviour of stratified liquid natural gas in storage tanks: a study of the rollover phenomenon, Int. J. Heat Mass Transfer 40 (1997) 1875–1884.

[17] M.A. Cotter, E.C. Michael, Transient cooling of petroleum by natural convection in cylindirical storage tanks—I. Development and testing of a numerical simulator, Int. J. Heat Mass Transfer 36 (1993) 2165–2174.

[18] M.A. Cotter, E.C. Michael, Transient cooling of petroleum by natural convection in cylindirical storage tanks—II. Effect of heat transfer coefficient, aspect ratio and temperature-dependent viscosity, Int. J. Heat Mass Transfer 36 (1993) 2175–2182.

[19] J. Ziotko, E. Supernak, G. Mojzesowicz, Transport and storage of oil and some aspects of ecology, J. Construct. Steel Res. 46 (1998) 290.

[20] B.E. Launder, D.B. Spalding, The numerical computation of turbulent flows, Comput. Methods Appl. Mech. Eng. 3 (1974) 269–289.

[21] J.L. Lage, A. Bejan, R. Anderson, Removal of contaminant in a slot ventilated enclosure, Int. J. Heat Mass Transfer 35 (1992) 1169–1179.

[22] C.-Y. Chow, An Introduction to Computational Fluid Mechanics, John Wiley, Canada, 1979.

[23] S. Torii, T. Yano, F. Tuchino, Heat transport in turbulent parallel Couette flows in concentric annuli for various Prandtl numbers, in: Proceedings of the 3rd International Thermal Energy Congress, Kitakyushu, Japan, pp. 209–214, 1997.